of a detailed model of this complex the ionization potential[10] of O^{+3}, 77 eV, constitutes an estimate for E_L. It is harder to estimate E_K, which must be greater than the K-shell binding energy[11] 532 eV in the isolated O atom but much smaller than the ionization potential[10] of O^{+6}, 739 eV. A rough estimate of E_K can be obtained with the aid of Larkins's calculations[12] of K-shell binding energies in neon for various degrees of ionization in the valence shell. These calculations predict that the K-shell binding energy is about 38% larger for Ne^{+8} (no L electrons) than for neutral neon. This percentage change agrees closely with the 39% increase in oxygen K-shell binding energy for complete removal of the L-shell electrons. Further, Larkins finds that after removal of half the neon L-shell electrons, the K-shell binding energy increases about 15%. If we assume the same percentage increase in oxygen K-shell binding energy after removal of half the oxygen L-shell electrons, we can estimate E_K for O^{+3} to be about 600 eV. Then $E_K - E_L$ is about 520 eV, an approximate result that agrees qualitatively with the experimental value 454 ± 30 eV.

The results presented in this paper are consistent with an earlier report[2] of 200-keV Q_{4T} distributions (where the T stands for "total") that were exceptionally wide compared to Q_{3T} and Q_{2T} distributions at the same energy. It is now clear that the Q_{4T} distributions were widened because they contained double peaking that was obscured by the poorer resolution available to those measurements.

ACKNOWLEDGMENTS

It is a pleasure to thank Robert E. Auer for maintaining the accelerator and collecting most of the data presented here.

*Work supported by the U. S. Atomic Energy Commission.

[1]F. W. Bingham, Phys. Rev. 182, 180 (1969).

[2]F. W. Bingham, Phys. Rev. A 2, 1365 (1970).

[3]F. W. Bingham and J. K. Rice, Phys. Rev. A 4, 996 (1971).

[4]U. Fano and W. Lichten, Phys. Rev. Letters 14, 627 (1965).

[5]W. Lichten, Phys. Rev. 164, 131 (1967).

[6]Q. C. Kessel, in *Case Studies in Atomic Collision Physics I*, edited by E. W. McDaniel and M. R. C. McDowell (North-Holland, Amsterdam, 1969), pp. 401–462.

[7]The screened Coulomb potential was used to calculate r_0 [see F. W. Bingham, J. Chem. Phys. 46, 2003 (1967)].

[8]J. P. Chandler, program STEPIT available from Quantum Chemistry Program Exchange, Department of Chemistry, Indiana University, Bloomington, Ind.

[9]J. S. Briggs and J. Macek, J. Phys. B 5, 579 (1972).

[10]C. W. Allen, *Astrophysical Quantities*, 2nd ed. (Athlone, London, 1963), pp. 37–40.

[11]J. A. Bearden and A. F. Burr, Rev. Mod. Phys. 39, 125 (1967).

[12]F. P. Larkins, J. Phys. B 4, 14 (1971).

PHYSICAL REVIEW A VOLUME 6, NUMBER 5 NOVEMBER 1972

Charge Transfer at Large Internuclear Distances: Application to Asymmetric Alkali-Ion–Alkali-Atom Systems*

Ronald E. Olson
Stanford Research Institute, Menlo Park, California 94025
(Received 30 June 1972)

Numerical coupled-channel two-state calculations have been employed to yield a reduced-total-cross-section curve as a function of reduced velocity for the case where the potential curves lie parallel to one another and there is an exponential coupling between them. This plot may be used to estimate the energy dependence of the charge-transfer inelastic total cross sections for transitions that occur at large internuclear distances due to coupling between two close-lying states. We have specifically applied the above plot to several alkali-ion–alkali-atom systems and find reasonable agreement between theory and experiment. The velocity at which the total cross sections reach their maximum is obtained for the general case and is found to be in fair agreement with experiment. A comparison between the results of Demkov and these calculations is also made.

I. INTRODUCTION

In the problem of understanding the energy dependence of charge-transfer inelastic total cross sections for the reaction

$$A^+ + B \rightarrow A + B^+ + \Delta E \quad , \tag{1}$$

there generally exist two different types of mechanism for the charge transfer.

The first mechanism is due to the crossing of

potential-energy curves, with the charge transfer occurring at the curve crossing. This type of mechanism predominates in the cases where the energy separation of the reactants and products at infinite internuclear separations is large. The curve-crossing case has been extensively explored in terms of the Landau–Zener–Stückelburg theory, and its limitations and regions of usefulness are now relatively well understood.[1]

A second type of mechanism can also exist that will give rise to large cross sections. This occurs for systems in which several potential curves lie very close together at large separations. Here, charge transfer occurs not because of a localized curve crossing but because the coupling between the states is comparable in magnitude to the potential-energy separation. A theoretical framework in which to study this very important class of reactions has been presented by Demkov.[2]

Many reactions fit into this last category, but probably the best studied experimentally are the alkali-ion–alkali-atom charge-transfer cross-section measurements of Perel and Daley.[3] These are also ideal systems for a theoretical study, because in most of the cases only two states, the reactant and product channels, dominate the charge-transfer reaction. Also, because there exists such a wealth of data on these relatively simple systems, theory is forced to understand them before going on to more complicated multichannel problems.

In this paper, we are concerned with the problem of charge transfer at large distances for the general two-state case. The cross sections and velocity are presented in terms of reduced units so that one common plot may be conveniently applied to this whole class of reactions. The results are tested against the measurements of Perel and co-workers on several alkali-ion–alkali-atom systems, and reasonable agreement is found between theory and experiment. Moreover, the parametrization of the position of the cross-section maximum is easily understood within this theory and agrees well with experimental measurements. A comparison with the results of using the Demkov formula is also made. We find the Demkov formula tends to underestimate the cross sections in the threshold energy region because of the neglect of the important region of coupling at large impact parameters.

II. THEORY

We are dealing here with the problem of charge transfer at large distances between two close-lying states. The formalism is very different from the Landau–Zener curve-crossing case where we assume a linear crossing of two potential-energy curves and a constant coupling-matrix element $H_{12}(R)$. Here, in essence, we have the opposite problem. The two potential curves are assumed to be parallel with one another, and the coupling-matrix element is assumed to have an exponential R dependence. The charge transfer at low to moderate energies is then found to be localized at the internuclear separation where the difference in potential curves is equal to twice the coupling-matrix element $H_{12}(R)$.

Stückelberg[4] first looked at this problem for the case where the coupling-matrix element has the form C/R^s. This form is important in excitation transfer for an optically allowed transition, $s=3$, or for a forbidden transition associated with a $(s-1)$-pole moment. Demkov, however, has specifically examined the charge-transfer case using an exponentially decreasing coupling-matrix element.[2] We will briefly review the theory of Demkov, then show how its accuracy may be significantly increased by using model numerical close-coupled calculations.

For charge transfer between a positive ion and an atom, the intermolecular potentials at large distances may be written as

$$V_i(R) = V_i(\infty) - \alpha_i/2R^4 \quad , \tag{2}$$

where α_i is the dipole polarizability of the neutral atom and $i=1, 2$ for the reactant and product states, respectively. Transfer of charge occurs in the region R_c where the coupling-matrix element $H_{12}(R)$ equals one-half the difference between the intermolecular potentials:

$$H_{12}(R_c) = \tfrac{1}{2}\left| V_1(R_c) - V_2(R_c)\right| = \tfrac{1}{2}\Delta V(R_c) \quad . \tag{3}$$

Over the region of transfer, $R_c \pm \Delta R_c$, it is a good approximation to set the coupling-matrix element equal to the simple exponential form

$$H_{12}(R) = e^{-\lambda R} \quad . \tag{4}$$

The transition probability can then be calculated as a function of impact parameter using the Demkov formula

$$P(b) = \operatorname{sech}^2\left(\frac{\pi \Delta V(R_c)}{2\hbar\lambda v(b)}\right) \sin^2\left(\frac{1}{\hbar}\int_{-\infty}^{\infty} H_{12}\,dt\right) \quad . \tag{5}$$

Here, all quantities are in atomic units, and the radial velocity at a specific impact parameter is given by

$$v(b) = v_0\left(1 - \frac{V_1(R_c)}{E} - \frac{b^2}{R_c^2}\right)^{1/2} \quad , \tag{6}$$

where v_0 is the incident velocity. Equation (5) is accurate for impact parameters $b \ll R_c$. Therefore, Eq. (5) neglects an important region of transfer for impact parameters $b \gtrsim R_c$.

Duman[5] has used the Demkov formula to calcu-

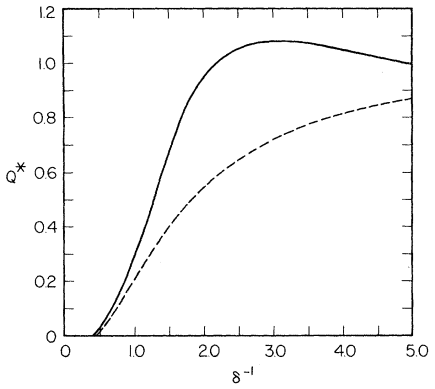

FIG. 1. Reduced total cross section Q^* [Eq. (14)] vs reduced velocity δ^{-1} [Eq. (13)]. The solid line is from numerical calculations, and the dashed line is from the Demkov formula.

late the cross sections for near-resonant charge exchange between He^+ ions and alkali atoms. He has simplified Eq. (5) by using two limiting forms for the cross sections. The first form, applicable to low collision energies, i.e., the threshold energy region for the cross sections, is given by

$$Q = \tfrac{1}{2}\pi R_c^2 f(v) \quad , \tag{7}$$

where

$$f(v) = \int_0^{R_c} \operatorname{sech}^2\left(\frac{\pi \Delta V(R_c)}{2\hbar\lambda v(b)}\right) d\left(\frac{b^2}{R_c^2}\right) \quad . \tag{8}$$

The second form, which is applicable at high energies, is identical with the formula used for resonant charge exchange. The Smirnov method is used for calculating the cross sections, [5] and it is found that

$$Q = \tfrac{1}{2}\pi R_0^2 \quad , \tag{9}$$

where R_0 is the solution to

$$\frac{1}{v_0}\left(\frac{2\pi R_0}{\lambda}\right)^{1/2} \frac{H_{12}(R_0)}{\hbar} = 0.28 \quad . \tag{10}$$

We have derived Eqs. (7) and (8) in a different way and find an equivalent form for the cross section:

$$Q = 4\pi R_c^2 \left(1 - \frac{V_1(R_c)}{E}\right) \int_1^\infty \frac{dx\, e^{-\delta x}}{x^3(1+e^{-\delta x})^2} \quad , \tag{11}$$

where

$$\delta = \frac{\pi \Delta V(R_c)}{2\hbar\lambda v_0}\left(1 - \frac{V_1(R_c)}{E}\right)^{-1/2} \quad . \tag{12}$$

For the type of ion-atom charge-transfer calculations considered here, it is an excellent approximation to set $[1 - V_1(R_c)/E]^{1/2}$ equal to unity, which is what we will do in the rest of this paper.

The important fact to be seen from the derivation of Eqs. (11) and (12) is that the cross sections in the threshold region can be represented in terms of a reduced velocity

$$\delta^{-1} = 2\hbar\lambda v_0/\pi \Delta V(R_c) \tag{13}$$

and in terms of a reduced cross section

$$Q^* = Q/\tfrac{1}{2}\pi R_c^2 \quad . \tag{14}$$

We have explored, using numerical calculations, the applicability of using a reduced plot of Q^* as a function of δ^{-1} to estimate the total cross sections. Numerical calculations are necessary here since the Duman formulas [Eqs. (7)–(10)] neglect the transitions occurring around and outside R_c. This, as will be shown in Sec. III, causes the total cross sections to be seriously underestimated in the threshold energy region. Variations in the parameters $\Delta V(R_c)$, λ, and R_c were made to see if one common curve could represent various starting conditions and also to determine the region of validity of the reduced curve.

III. REDUCED CROSS SECTIONS

The numerical calculations of the transition probabilities that are required to compute the reduced cross sections were performed using the semiclassical forced-turning-point method of Bates and Crothers. [6] The singularity at the turning point was removed by utilizing the change of variables suggested by Bates and Sprevak. [7]

Various combinations of $\Delta V(R_c)$, λ, and R_c were used to test the validity of employing a common reduced-cross-section curve. $\Delta V(R_c)$ was varied from 0.006 to 0.1 a.u. (0.16 to 2.7 eV), λ from $0.3a_0^{-1}$ to $0.6a_0^{-1}$, and R_c from $7.5a_0$ to $16a_0$. The solid line on Fig. 1 depicts the calculation of the reduced cross section Q^* vs the reduced velocity δ^{-1}. In the range of reduced velocity shown, the solid line is within 10% of all calculations. A numerical summary of the solid line of Fig. 1 is given by Table I. The dashed line on Fig. 1 is the evaluation of the Demkov equation using the low-energy formula [Eqs. (7) and (8)]. We find a considerable difference between the numerical calculations and the low-energy Demkov formula.

TABLE I. Calculated reduced cross sections.

δ^{-1}	Q^*
0.5	0.03
1.0	0.30
1.5	0.66
2.0	0.95
2.5	1.05
3.0	1.08
3.5	1.07
4.0	1.05
4.5	1.02
5.0	0.99

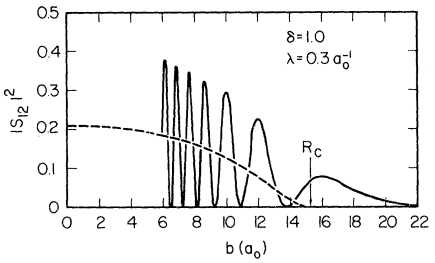

FIG. 2. Transition probabilities vs impact parameter for $\delta = 1.0$, $\lambda = 0.3a_0^{-1}$, $\Delta V(R_c) = 0.02$ a.u., and $R_c = 15.35a_0$. The solid line is from numerical calculations, and the dashed line is from the Demkov formula.

Around $\delta^{-1} = 2.0$, this difference amounts to almost a factor of 2.

The reason for the large difference between the numerical calculations and the Demkov formula lies in the fact that the transition probability formula given by Eq. (5) does not accurately take into account the transitions occurring at impact parameters $b \gtrsim R_c$. The transitions occurring here have a considerable effect on the cross-section magnitude, since the transition probability is weighted by the impact parameter in the cross-section integral

$$Q = 2\pi \int_0^\infty db\, bP(b) \quad . \tag{15}$$

The neglect of transitions occurring around $b \gtrsim R_c$ causes the cross sections to be underestimated.

A comparison between the Demkov low-energy formula [Eqs. (7) and (8)] and numerical calculations for the transition probabilities is shown in Fig. 2. For this comparison, $\delta = 1.0$, $\lambda = 0.3a_0^{-1}$, $\Delta V(R_c) = 0.02$ a.u., and $R_c = 15.35a_0$. The numerical transition probabilities possess oscillations due to the interference between the two possible trajectories at a given impact parameter. In this case, for impact parameters $b \lesssim 10a_0$, the random-phase approximation may be used to calculate the cross section. In this approximation, the rapidly oscillating transition probabilities are set equal to their average value. When the random-phase approximation is applied to the numerical results shown in Fig. 2, we find good agreement for $b \lesssim 10a_0$ with the low-energy Demkov formula (the dashed line) derived by setting the $\sin^2(\ )$ term of Eq. (5) equal to $\frac{1}{2}$. In our calculations of the cross sections we have used the Demkov formula [Eqs. (7) and (8)] at small impact parameters where the transition probabilities are oscillating rapidly. Numerical checks indicate that the Demkov formula is very accurate for low impact parameters and for rapidly oscillating transition probabilities.

In Fig. 2 the main difference between the cross section calculated from transition probabilities obtained from the Demkov formula and those from the numerical calculations arises from the transition probabilities around $b \approx R_c$. There is a considerable amount of tunneling outside of R_c which greatly increases the cross section. For the example shown by Fig. 2, the Demkov formula underestimates the reduced cross section with a value equal to 0.202, while the numerical calculations yield $Q^* = 0.317$.

At reduced velocities greater than $\delta^{-1} \gtrsim 5$, the reduced curve shown in Fig. 1 cannot be used to estimate the cross sections. At the higher velocities the collision behaves as if the system is resonant and a new set of parameters is needed to represent the collision process. From Eqs. (9) and (10) we see these parameters are the collision velocity and λ, the exponential decay factor of $H_{12}(R)$. In Fig. 3 are shown the cross sections obtained by varying λ, Eqs. (9) and (10). This formulation, which strictly applies to resonant charge exchange, is accurate at the higher velocities where Fig. 1 is no longer applicable. In practice, we find that the high-energy cross sections join with the cross sections calculated from Fig. 1 at around $\delta^{-1} \approx 5.0$.

IV. APPLICATIONS

A. $Li^+ + Na$

Two of the simplest systems to study theoretically are the charge-transfer reactions

$$Li^+ + Na \rightarrow Li + Na^+ + 0.25 \text{ eV} \quad , \tag{16}$$

$$Na^+ + Li \rightarrow Na + Li^+ - 0.25 \text{ eV} \quad . \tag{17}$$

These reactions proceed primarily via the two ground states. The nearest excited state is excitation to Li(2p) in reaction (16), which has a ΔE of -1.60 eV and only slightly affects the magnitude of this cross section. Both of the above

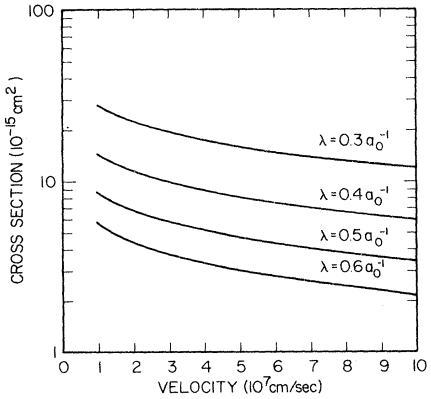

FIG. 3. High-energy cross sections vs the coupling parameter λ.

reactions have been measured experimentally by Daley and Perel[8] so that it is possible to test the validity of any theoretical technique.

In order to calculate the cross sections, it was first necessary to estimate the internuclear separation at which charge transfer occurs, i.e., $\Delta V(R_c) = 2H_{12}(R_c)$. The calculation of $\Delta V(R)$ was performed using Eq. (2) with spectroscopic energy levels, and the theoretical dipole polarizabilities obtained from the paper by Dalgarno and Kingston.[9] The coupling-matrix element calculation was performed using the formula[10]

$$H_{12}(R) = I_1^{1/2} I_2^{1/2} R^* e^{-0.86R^*} , \tag{18}$$

where

$$R^* = \tfrac{1}{2}(\alpha + \gamma)R . \tag{19}$$

In Eq. (19), $\frac{1}{2}\alpha^2$ equals the effective ionization potential of the atom of Eq. (1) in the reactant state, and $\frac{1}{2}\gamma^2$ equals the effective ionization potential of the atom in the product state with all quantities being in atomic units. In essence, the $H_{12}(R)$ used here means that the cross sections calculated for reactions (16) and (17) will be identical within the two-state approximation.

Using the above formulas, we find that the critical distance at which charge transfer occurs, or where the wave functions change from an atomic to a molecular basis, is $R_c = 10.63a_0$. Here $\Delta V(R_c)$ of Eq. (3) is equal to 0.00922 a.u.

In a recent paper by Bottcher and Oppenheimer,[11] the authors have calculated *ab initio* potential curves for $LiNa^+$ and state that they find a curve crossing at $R = 10.8a_0$. The cross sections computed from the potential curves are then explained in terms of a curve-crossing model. This explanation seems very unlikely, however, since the long-range dipole polarizabilities for Li and Na are almost identical,[9] so that $\Delta V(R)$ will be essentially equal to ΔE for internuclear separations around $10a_0$ to $11a_0$. The change in character of the wave functions that the authors[11] attribute to a curve crossing is most likely the simple type of long-range interaction being studied in this paper.

The only other quantity needed to calculate the cross sections is $\lambda = 0.56a_0^{-1}$ [Eq. (4)] which is determined from the coupling-matrix element [Eq. (18)] at R_c. The replacement of the form of Eq. (18) by Eq. (4) is valid since the charge transfer occurs over a narrow range of R centered about R_c. Using Eqs. (13) and (14) and Figs. 1 and 3, it is now possible to calculate the cross sections and compare them with experiment. The results are shown in Fig. 4. The threshold and position of the maximum of the experimental cross sections are well reproduced by theory. The magnitude of the cross sections are about 30% below the experimental ones, which probably indicates that the coupling-matrix element H_{12} as given by Eq. (18) is below the true value by about 50%. H_{12} could be adjusted to give an almost perfect fit to the data but this would not test the limitations of the theory.

The oscillations on the cross sections for the nonresonant alkali-ion–alkali-atom charge-transfer systems have been explained in a previous paper as due to a nonrandom-phase contribution to the cross sections caused by an extremum in the difference potential between the reactant and product states.[12] Such an extremum is found in the difference potential in the *ab initio* potential calculations of Bottcher and Oppenheimer at $R \approx 4a_0$ which does explain the frequency of the observed oscillations. The explanation given in Ref. 11 for the physical origin of the cross-section oscillations is different from the simple model proposed in Ref. 12. In this paper, however, we are not concerned with the oscillatory structure, but only with the over-all energy dependence of the cross sections.

The explanation for the slight difference in magnitude of the cross sections observed experimentally for the $Li^+ + Na$ and $Na^+ + Li$ systems can be explained as due to the influence of higher-lying inelastic channels. From the correlation diagrams of Barat and Lichten[13] it can be predicted that a Π-state potential leading to *np* excitation will cross the Σ-reactant-state potential for most of the exothermic alkali-ion–alkali-atom reactions, such as in the case of $Li^+ + Na$. A verification of this crossing in the $LiNa^+$ system is shown in the potential curves of Bottcher and Oppenheimer.[11] The Coriolis coupling between the Σ and Π states for curves crossing around $R \approx 6a_0$ can lead to an additional contribution to the cross sections for the exothermic reactions. An estimate of the magnitude of this cross section can be obtained from the work of McMillan on Li_2^+, who finds the Σ-Π cross section increasing from 0.2×10^{-15} to 1.0×10^{-15} cm^2 in the velocity region studied here.[14,15]

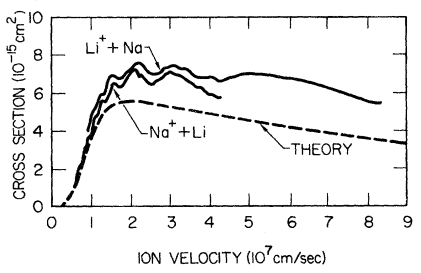

FIG. 4. $Li^+ + Na$ and $Na^+ + Li$ total charge-transfer cross sections. The solid lines are from the experiments of Daley and Perel (Ref. 8); the dashed line is from this theory.

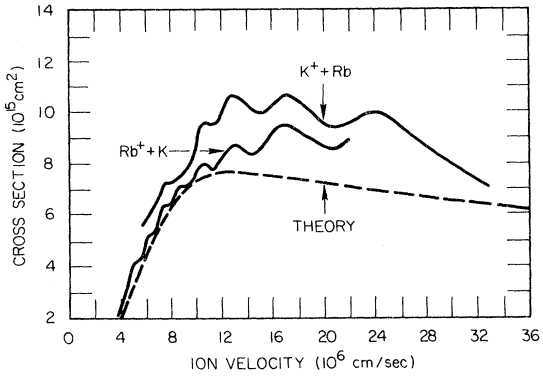

FIG. 5. $K^+ + Rb$ and $Rb^+ + K$ total charge-transfer cross sections. The solid lines are from the experiments of Perel and Yahiku (Ref. 15); the dashed line is from this theory.

B. $K^+ + Rb$

Calculations for the $K^+ + Rb$ and $Rb^+ + K$ charge-exchange cross sections have also been used for a comparison with the experimental data of Perel and Yahiku.[16] These systems, as in the previous case, can be handled effectively within a two-state framework. The energy separation at infinity is ± 0.163 eV, and the states lie parallel to one another at large separations.

The calculations were performed in an identical manner to the $Li^+ + Na$ system except that the input parameters such as dipole polarizabilities, energy levels, and matrix elements were changed to reflect this system. The charge transfer was found to occur at $R_c = 12.50a_0$ where the potential-energy difference $\Delta V(R_c)$ was equal to 0.00568 a.u. The coupling-matrix element [Eqs. (4)] was characterized by $\lambda = 0.469a_0^{-1}$.

The results of the calculation and the experimental data are shown in Fig. 5. Again the calculations underestimate the experimental cross sections in the area of the maximum, but reproduce the threshold region. For both the $Rb^+ + K$ and $K^+ + Rb$ charge-transfer reactions the theory predicts identical cross sections. The experiment shows the $K^+ + Rb$ cross sections to be larger than the $Rb^+ + K$. We explain this as due to the additional contribution of excitation to the $K(4p)$ state from Coriolis coupling between the ground Σ state and the Π state leading to $K(4p)$. Detailed *ab initio* potential calculations will, however, be necessary to substantiate this claim.

C. $Li^+ + K$

The $Li^+ + K$ system poses a more difficult problem, because the reaction is dominated by the two processes

$$Li^+ + K \rightarrow Li(2s) + K^+ + 1.05 \text{ eV} , \qquad (20a)$$

$$Li^+ + K \rightarrow Li(2p) + K^+ - 0.80 \text{ eV} . \qquad (20b)$$

The theory presented above is not directly applicable to a three-state system; however, it can give a good estimate of the relative importance for both processes of Eq. (20). Moreover, we estimate that the derived cross sections for each process will be approximately 30% too large at the cross-section maximum due to the neglect of the coupling to the competing channel. At the threshold energies the sum of the cross sections for the two separate processes of Eq. (20) will give the same result as a three-state calculation. However, around the cross-section maximum the sum of the individual cross sections will overestimate the true result by about 30%. This figure is estimated from the transition probabilities that give a maximum value for an n-state process as $(n-1)/n$, neglecting phase effects.

In the calculations we find the region of coupling for both processes is centered around $R_c = 8.30a_0$. At first glance, one would expect the coupling to the excited state of Eq. (20b) would occur at a larger separation than the ground state and hence give rise to a larger cross section. However, when the long-range R^{-4} potential is included in the calculations, both processes are given equal weight since the polarizability of $Li(2s)$ is $165a_0^3$ and $K(4s)$ is $281a_0^3$. The polarizability of $Li(2p)$ will be larger than that of $Li(2s)$, and, as an estimate, we have set it equal to the polarizability of $K(4s)$. For reaction (20a) the pertinent parameters are $\Delta V(R_c) = 0.0264$ a.u. and $\lambda = 0.522a_0^{-1}$, and for reaction (20b) the parameters are $\Delta V(R_c) = 0.0293$ a.u. and $\lambda = 0.509a_0^{-1}$.

The results of the calculations are shown in Fig. 6. It was found that the cross sections for each of the processes of Eq. (20) were identical. They are shown by the dot-dashed line labeled "theory $\sigma(2p)$." The total cross section, which is simply double the $\sigma(2p)$ curve, is given by the long-dashed line. We estimate that this curve is too large by 30% at the maximum, so that theory would again underestimate the magnitude of the experimental cross sections[3] (solid line) around the maximum.

Although the theoretical total cross section for all processes is in reasonable agreement with experiment, there is a serious difference between theory and experiment as to the cross section leading to $Li(2p)$ excitation. Possibly the reason for the discrepancy in the magnitude and shape for this cross section lies in the fact that the theory should only be applied to S-state atoms and its use here is invalid. Since only Σ-Σ interactions are included by this theory, the neglect of the Σ-Π transition to $Li(2p)$ can lead to erroneous results.[17] Another possibility for the discrepancy in magnitude is that the optical experimen-

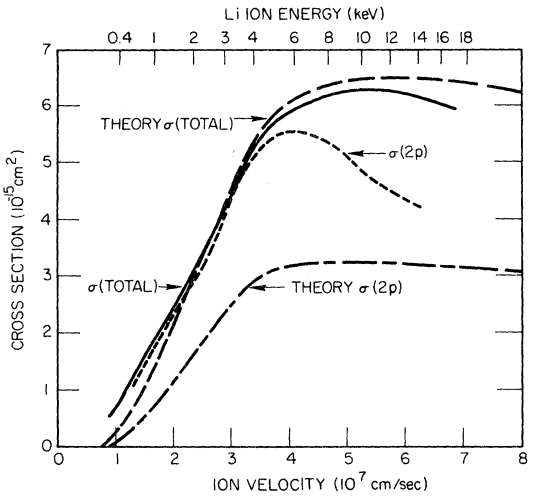

FIG. 6. $Li^+ + K$ total charge-transfer cross sections. The solid line is the experimental total cross section; the short-dashed line labeled $\sigma(2p)$ is the experimental cross section for excitation to the Li($2p$) state (Ref. 3). The theoretical total cross section is given by the long-dashed line, and the cross section for excitation to the Li($2s$) and Li($2p$) states is shown by the line labeled "theory $\sigma(2p)$."

tal values for the $2p$ cross sections are not absolute, but have been normalized to the slope of the total-cross-section curve. This procedure yields a cross-section curve for Li($2p$) excitation that can only be considered an upper limit to the true Li($2p$) cross sections. Possibly some of the factor-of-2 difference between theory and experiment is due to this normalization procedure. The lack of agreement in the shape of the Li($2p$) cross section around the maximum is an unsettling factor for the theory. One possible explanation for the rapid decrease in the experimental cross section above 4×10^7 cm/sec is simply the onset of oscillations similar to those observed on other alkali systems. Since this theory does not predict any oscillations, this type of structure would not be expected on the theoretical curve.

D. Cross-Section Maximum

Another problem that the theory can address itself to is the velocity at which the cross sections rise to their maximum. Perel and Daley[3] were able to parametrize the experimental results by the form

$$v_{\max} = a|\Delta E|/I^{1/2} \quad , \tag{21}$$

where a equals 22×10^7 for low-ΔE processes and has a parabolic form for the higher-ΔE processes. It appears, however, that the higher-ΔE systems also have a linear dependence but with a slope equal to 8×10^7.

The reduced cross sections shown in Fig. 1 may be applied to this problem, and we find the maximum cross section occurs when

$$\delta^{-1} = 2\hbar\lambda v_{\max}/\pi\Delta V(R_c) = 3.1 \quad . \tag{22}$$

Several approximations are now necessary to arrive at an equation similar to (21). First, we must neglect the polarization potentials and assume that

$$\Delta V(R) = |\Delta E| \tag{23}$$

in the region of charge transfer; that is, assume that the polarizabilities of the reactant and product systems are not very much different. Second, a form for λ must be found. The semiempirical result of Rapp and Francis[18] can be used for the exponential coupling term with

$$\lambda \approx [I(\text{eV})/13.6]^{1/2}, \tag{24}$$

where I is the ionization potential of the electron to be transferred. Equations (23) and (24) may now be substituted into (22) with the result

$$v_{\max} = 14.5\times10^7(\Delta E/I^{1/2})\,(\text{cm/eV}^{1/2}\,\text{sec}). \tag{25}$$

The theoretical result, (25), is shown by the dashed line in Fig. 7. There is reasonably good agreement with experiment considering the nature of the approximations [Eqs. (23) and (24)]. Differences between theory and experiment should be expected with the parametrization given by (21), since $\Delta E = \Delta V(\infty)$ is only a convenient approximation to the necessary parameter $\Delta V(R_c)$. Also, the coupling-term parameter λ should reflect both the initial and final states of the electron being transferred in reaction (1).

V. CONCLUSIONS

The method of Demkov[2] has been used to parametrize the results of numerical total-cross-section calculations for systems where charge transfer takes place between two close-lying parallel potential curves. The results may be applied to a great number of systems. As examples, several alkali-ion–alkali-atom systems were chosen for a comparison with theory. It was found that there was reasonable agreement with experiment, with the threshold cross sections well reproduced and the maximum position in agreement. The theoretical results, however, tended to underestimate the experimental cross sections by approximately 30% which probably indicates that the coupling-matrix element should be increased by 50% at large internuclear separations.

The low-ΔE formula used by Perel and Daley[3] to parametrize the experimental results on the velocity at which the cross sections reach a maximum [Eq. (21)] has been justified in this work. The value for the parameter a of (21) obtained from the theoretical work is found to be in reasonable agreement

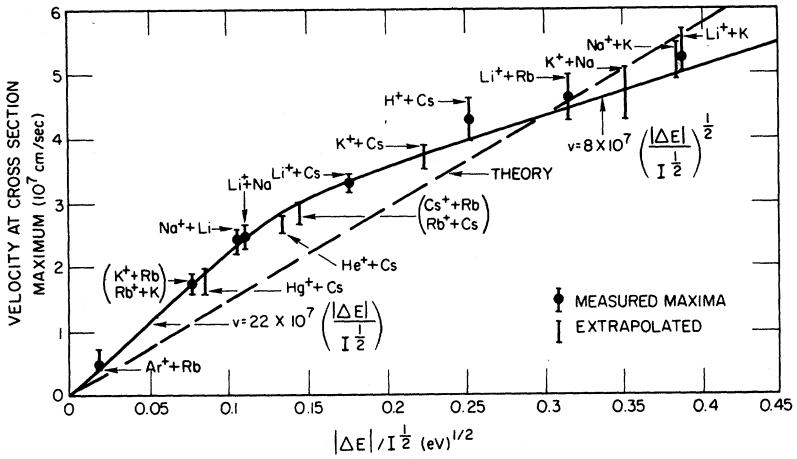

FIG. 7. Velocity at the cross-section maximum vs $|\Delta E|/I^{1/2}$ taken from Fig. 1 of the paper by Perel and Daley (Ref. 3). The dashed line is the theoretical prediction of the cross section maximum.

with experiment. The nature of the approximations needed to arrive at (21) have also been elucidated. This same functional form has been obtained by Drukarev,[19] who was not able to estimate the value of the slope for this equation.

One disagreement with experiment lies in the magnitude of the Li(2p) cross section for the $Li^+ + K$ reaction [Eq. (20)]. Although there is agreement as to the magnitude of the total cross section for all processes, theory predicts a smaller cross section than experiment for the Li(2p) contribution. The difference may be due to an inadequacy in the theory, or due to the normalization of the experimental optical cross section to the slope of the total cross section.

For many of experimentally observed cross sections where both the $A^+ + B$ and $A + B^+$ cross sections have been measured, it is found that the exothermic reaction has a slightly larger cross section. Within a two-state theoretical framework we would expect both cross sections to be identical. However, from the work of Barat and Lichten,[13] it is evident that there will be a curve crossing between the gound Σ state and an excited Π state that leads to the products of the exothermic reaction for many alkali systems. The magnitude of this cross section can be estimated from the work of McMillan[14] and is close to the difference in cross sections observed in experiments. The contribution of this additional state therefore will slightly increase the cross sections for the exothermic reaction. We expect that the above reason explains the difference in magnitude of the cross sections for the $Li^+ + Na$ and $Na^+ + Li$ reactions and for the $K^+ + Rb$ and $Rb^+ + K$ reactions. Experimentally, this hypothesis may be tested by looking for the optical emission from the particular np state.

The oscillations observed experimentally on the cross sections for alkali charge-transfer systems have not been a topic of this paper. The explanation has been given in a previous paper.[12] The oscillations are due to nonrandom contributions to the phases in the cross-section calculation caused by one or more extrema in the difference between the potentials for the product and reactant states. This explanation is different from, and should not be confused with, that given by Rosenthal and Foley[20] to explain (correctly) the total-cross-section oscillations observed optically on many highly nonresonant systems such as He_2^+.

ACKNOWLEDGMENTS

The author would like to thank Dr. Felix Smith and Dr. Donald Lorents for their helpful comments and suggestions in the preparation of this manuscript.

*Work supported by the Office of Naval Research.

[1]See, for example, D. R. Bates, Proc. Roy. Soc. (London) A257, 22 (1960); J. B. Delos and W. R. Thorson, Phys. Rev. Letters 28, 647 (1972).

[2]Yu. N. Demkov, Zh. Eksperim. i Teor. Fiz. 45, 195 (1963) [Sov. Phys. JETP 18, 138 (1964)].

[3]See J. Perel and H. L. Daley, Phys. Rev. A 4, 162 (1971), and references therein.

[4]See the discussion in N. F. Mott and H. S. W. Massey, *The Theory of Atomic Collisions*, 3rd ed. (Oxford U. P., Oxford, England, 1965), pp. 651–652.

[5]E. L. Duman, *Seventh International Conference on the Physics of Electronic and Atomic Collisions*, 1971 (North-Holland, Amsterdam, 1971), p. 471.

[6]D. R. Bates and D. S. F. Crothers, Proc. Roy. Soc. (London) A315, 465 (1970).

[7]D. R. Bates and D. Sprevak, J. Phys. B 3, 1483 (1970). The denominator of one of the applicable equations [Eq. (20)] should be corrected to read $\{V_{1u}(R) + V_{2u}(R)\}\{R^2 - p(R)^2\rho^2\}^{1/2}$.

[8]H. L. Daley and J. Perel, *Sixth International Conference on the Physics of Electronic and Atomic Colli-*

sions, 1969 (MIT Press, Cambridge, Mass., 1969), p. 1051.

[9]A. Dalgarno and A. E. Kingston, Proc. Roy. Soc. (London) 73, 455 (1959).

[10]R. E. Olson, F. T. Smith, and E. Bauer, Appl. Opt. 10, 1848 (1971).

[11]C. Bottcher and M. Oppenheimer, J. Phys. B 5, 492 (1972).

[12]R. E. Olson, Phys. Rev. A 2, 121 (1970).

[13]M. Barat and W. Lichten, Phys. Rev. A 6, 211 (1972).

[14]W. L. McMillan, Phys. Rev. A 4, 69 (1971).

[15]As a note of proof, Melius and Goddard have investigated the effect of the Σ-Π crossing in the $Li^+ + Na$ reaction and also arrive at this same conclusion, C. F. Melius and W. A. Goddard III (private communication).

[16]J. Perel and A. Y. Yahiku, *Fifth International Conference on the Physics of Electronic and Atomic Collisions, Leningrad*, 1967 (Nauka, Leningrad, 1967), p. 400.

[17]C. F. Melius (private communication).

[18]D. Rapp and W. E. Francis, J. Chem. Phys. 37, 2631 (1962).

[19]G. F. Drukarev, *Fifth International Conference on the Physics of Electronic and Atomic Collisions, Leningrad*, 1967 (Nauka, Leningrad, 1967), p. 10.

[20]H. Rosenthal and H. M. Foley, Phys. Rev. Letters 23, 1480 (1969).

PHYSICAL REVIEW A VOLUME 6, NUMBER 5 NOVEMBER 1972

Ionization Cross Sections for H_2, N_2, and CO_2 Clusters by Electron Impact

Franco Bottiglioni, Jacques Coutant, and Mario Fois
Association Euratom-CEA Département de la Physique du Plasma et de la Fusion Contrôlée, Centre d'Etudes Nucléaires, Boîte Postale n°6, 92 Fontenay-aux-Roses, France
(Received 29 March 1972)

Clusters of condensed matter which are produced under some particular conditions in supersonic molecular jets can be ionized by electrons. Measured ionization cross sections show a sharp dependence on N, the mean number of molecules per cluster. For small clusters ($\bar{N} < 50$) the cross sections increase as N; for larger clusters as about $\bar{N}^{2/3}$. Furthermore the electron initial energy W_{eM}, for which the cross section is maximum, increases with N. In this paper we present a model for the computation of the cluster ionization cross sections which includes the energy losses inside the cluster of both primary and secondary electrons. The escape probability for secondary electrons is given as a function of their initial position and energy. This latter is related to the primary-electron energy. Results of these computations for H_2, CO_2, and N_2 clusters are in good agreement with experimental data.

I. INTRODUCTION

The formation of molecular clusters in free-expansion supersonic jets has been observed by Becker *et al.*[1] For gases such as CO_2, cluster formation occurs above a critical pressure even at room temperature. Permanent gases such as N_2 or H_2, on the contrary, must be near their liquefaction temperature before expansion in order to form clusters.

As shown by Raoult, Farges, and Rouault[2] and by Audit[3] these clusters have a crystalline structure, and their size is determined by the expansion parameters: pressure ratio, nozzle-skimmer distance, nozzle shape and size. Clusters are ionized (positive charge) by electron collisions[4-9] and can be accelerated up to high energies in electrostatic accelerators.[4-7]

The ionization cross section we are concerned with in this paper has to be defined. Because of ionization, the attenuation of a neutral cluster beam with intensity I_0 and velocity v_c, each cluster containing N molecules, which intersects an electron target, length dl, electron density n_e, electron velocity $v_e \gg v_c$, can be written as

$$dI_0 = -I_0 \sigma n_e (v_e/v_c) dl \ , \qquad (1.1)$$

where $\sigma(N, W_{e0})$ is the cluster ionization cross section and W_{e0} is the electron energy.

Measurements of σ are uneasy due to the spread in the cluster masses. Generally it is possible to measure the mean molecular mass number $\bar{N}$ of the cluster beam, without knowing $f(N)$, the distribution function of the cluster mass. The experimental cross section is related to $\bar{N}$. Therefore $\sigma_{expt}(\bar{N}, W_{e0})$ defined as in (1.1) is actually

$$\sigma_{expt}(\bar{N}, W_{e0}) = \sigma_{av}(N, W_{e0}) = \sum_{1}^{N_{max}} f(N)\sigma(N, W_{e0}) \Big/ \sum_{1}^{N_{max}} f(N) \ . \qquad (1.2)$$

Ionization cross sections for hydrogen clusters under electron impact have been measured by Tay[7]; for argon and CO_2 clusters by Falter *et al.*[8] These cross sections are measured at a given electron energy as a function of the mean value of the number of molecules per cluster.

The most important features of their results are the following: (a) At constant energy, the cross section is proportional to the mean mass number of the cluster $\bar{N}$ up to a critical value, roughly